The hydrogen bonding structure of water in the vicinity of apolar interfaces: a computer simulation study

2004 J. Phys.: Condens. Matter 16 S5389

(http://iopscience.iop.org/0953-8984/16/45/006)

INSTITUTE OF PHYSICS PUBLISHING JOURNAL OF PHYSICS: CONDENSED MATTER

J. Phys.: Condens. Matter **16** (2004) S5389–S5402 PII: S0953-8984(04)76337-7

The hydrogen bonding structure of water in the vicinity of apolar interfaces: a computer simulation study

Pál Jedlovszky

Department of Colloid Chemistry, Eötvös Loránd University, Pázmány Péter sétány 1/a, H-1117 Budapest, Hungary

E-mail: pali@para.chem.elte.hu

Received 19 February 2004
Published 29 October 2004
Online at stacks.iop.org/JPhysCM/16/S5389
doi:10.1088/0953-8984/16/45/006

Abstract

The structure and energetics of water–water hydrogen bonding has been analysed in detail in the vicinity of the water/vapour, water/CCl_4 and water/1,2-dichloroethane interfaces on the basis of Monte Carlo computer simulations. The dependence of various characteristics of the water–water hydrogen bonding, such as the interaction energy of the hydrogen bonded water pairs, the geometry (i.e. distance and angle) of the hydrogen bonds, the spatial arrangement of the neighbouring molecules around each other, and the population of the hydrogen bonded and coordinating neighbours on the distance from the interface has been investigated.

It has been found that the water–water hydrogen bonds are, on average, slightly more bent and longer in the interfacial region than in the bulk phase. The latter difference is due to the decrease of the population of the closest approaching water pairs, which correspond also to the largest Lennard-Jones repulsion, and hence the above changes of the hydrogen bond geometry are accompanied by a noticeable lowering of the average interaction energy of the hydrogen bonded water pairs at the vicinity of the interface. The number of the hydrogen bonded neighbours as well as of those belonging to the first coordination shell decreases, while the probability of two neighbours forming large angles around the central molecule becomes smaller upon getting closer to the interface. The overall structure of water is found to be more tetrahedral at the vicinity of the interface than in the bulk liquid phase.

1. Introduction

Hydrophobic hydration [1] is a phenomenon that plays a key role in the formation of various complex mesoscopic assemblies, such as micelles, bilayer membranes and lamellar systems,

and also various biological structures (e.g., cell membranes, membrane-bound proteins, etc). The structure of water changes in the vicinity of hydrophobic objects, resulting in an effective attraction of the apolar solutes. Due to its importance in many areas of science, hydrophobic hydration is still a subject of intensive theoretical [2] and experimental investigations [3–6] as well as of computer simulation studies [6–10].

A limiting case of hydrophobic hydration, corresponding to the presence of an apolar solute of infinite size, is the behaviour of water at the vicinity of a planar hydrophobic wall. However, intensive scientific investigation of the molecular level structure of water at such interfaces has been hampered by the lack of appropriate experimental methods. The recent development of various experimental techniques (e.g., sum frequency generation and second harmonic generation spectroscopy, neutron and x-ray reflection, etc) has thus been followed by a large number of experimental studies [11–18], accompanied by theoretical works [19, 20] on interfacial water. In order to get an insight into the molecular level detail of the properties of interfacial water, these systems have also been studied in detail by computer simulation methods [21–38].

In analysing the effect of the apolar interface on the structure of water, the interface-induced orientational order of the water molecules has been the main focus of computer simulation investigations. However, different studies have often led to different conclusions about this point, some of which are clearly incompatible with each other. Among the numerous conclusions drawn, the following statements are now widely accepted:

(i) the dipole vector of the interfacial water molecules prefers to lay parallel with the interface [21, 23, 26];
(ii) the deviation of the water dipoles from this preferred alignment is such that the dipole vector of the water molecules located at the aqueous and those at the apolar side of the interface are more likely to point toward the aqueous and toward the apolar phase, respectively [25, 32];
(iii) the water molecules belonging to the first water layer adjacent to the apolar phase prefer to align in such a way that the vector joining their H atoms [23, 26] or one of their O–H bonds [30] is perpendicular to the interface, whereas
(iv) water molecules located behind this layer prefer to lay parallel with the plane of the interface [30].

Recently we have shown that interfacial water molecules have two distinct orientational preferences: the first of these preferred orientations, present in the entire interfacial region, is parallel with the interface, whereas in the other preferred orientation, which is present only among the water molecules located closest to the apolar phase, the molecular plane is perpendicular to the plane of the interface and one of the O–H bonds points straight toward the apolar phase [33, 34, 36, 37]. We have also demonstrated that the ambiguity of the conclusions drawn in previous studies originates in the inappropriate choice of the statistical variables used, as the existence of the dual orientational preference can only be revealed by calculating a bivariate joint probability distribution of two independent variables characterizing the orientation of the water molecules relative to the interface [33, 37].

In contrast to the orientational ordering of water molecules, relatively little attention has been paid to the investigation of the dependence of the water–water structure, in particular, that of the water–water hydrogen bonding, on the presence of a nearby apolar interface. The majority of the studies in which this point is also investigated are limited to the analysis of the change in the number of hydrogen bonding and coordinating neighbours of the water molecules. It has been found for interfaces between water and apolar liquids [21, 23, 32, 35] as well as for the liquid–vapour interface of pure water [23] and aqueous solutions [30] that

upon approaching the interface the number of both the hydrogen bonding and coordinating (i.e. belonging to the first coordination shell) neighbours of the molecules decreases, whereas their ratio increases (i.e. an increasing fraction of the coordinating neighbours form a hydrogen bond with the central water molecule). On the other hand, the characteristic features (e.g., peak and minimum positions) of the water atom–atom pair correlation functions are found to be practically unchanged at the vicinity of various water–apolar interfaces, and hence it has been concluded that the local structure of water is not affected by the presence of a nearby apolar interface [23, 26, 32]. However, only a few studies have gone beyond the level of the pair correlation functions in analysing the local structure of interfacial water. Among these studies, Linse has calculated several angular distributions in his pioneering work on the water–benzene interface [21]. He has found that the presence of a nearby interface suppresses the possibility of a linear dipole–dipole orientation of the neighbouring molecules as well as the spatial arrangement of two coordinating neighbours forming large angles around the central water molecule, enhancing the fraction of closely packed water trimers, whereas the angle of the water–water hydrogen bonds remains practically unchanged [21].

In the present study we perform a comprehensive analysis of the hydrogen bonding structure of water at the vicinity of various apolar interfaces. Thus, the geometry and the energetic properties of the hydrogen bonded water pairs as well as hydrogen bonding statistics are analysed in detail at different distances from the interface. Three different interfacial systems are investigated: the liquid–liquid interface formed by water with an apolar and a weakly polar liquid, i.e. carbon tetrachloride and 1,2-dichloroethane (DCE), respectively, and the water liquid–vapour interface. The results are compared to those obtained in the bulk liquid water region of the systems. The paper is organized as follows. In the next section details of the simulations performed are given. Then the obtained results are discussed in detail. Finally, some conclusions are drawn.

2. Computational details

Monte Carlo simulation of three systems, each of them containing an interface between liquid water and an apolar phase, has been performed on the canonical (N, V, T) ensemble at 300 K. The first system contained the liquid and vapour phases of water, whereas in the other two systems the apolar phase was neat liquid CCl_4 and DCE, respectively. The two organic liquids chosen correspond to rather different molecular polarities: while CCl_4 is a nearly spherical, apolar molecule, DCE is moderately polar, having a liquid phase dielectric constant of about 10 [39]. The simulations were performed in a rectangular basic simulation box. The length of its edge perpendicular to the interface X was 50.432 Å, whereas the Y and Z edges were both 25.216 Å long. Standard periodic boundary conditions have been used. The aqueous phase of each system consisted of 536 water molecules, described by the SPC/E potential model [40]. In order to check the sensitivity of the obtained results on the water model used, we have repeated the simulation of the system containing the water liquid/vapour interface using the TIP4P water model [41] instead of SPC/E. No considerable difference has been found between the results obtained in the systems of different water models. The CCl_4 and DCE phases have contained 98 and 120 molecules, respectively. The number of the molecules of each type has been determined in such a way that the density of the corresponding liquid phase at atmospheric pressure, confined to the space half of the volume of the basic simulation box, is reproduced. The DCE molecules have been described by a rigid version of the potential model of Benjamin [23], in which all bond lengths and bond angles have been fixed at their equilibrium values. In order to take the *trans*/*gauche* equilibrium of the molecules into account in a simple and computationally efficient way, the geometry of 80 DCE molecules has been

set to the *trans*, and that of the other 40 molecules to the *gauche* conformation, reproducing the experimental *trans*/*gauche* ratio of 2:1 [42]. For the description of the CCl_4 molecules a five-site Lennard-Jones model [43] was used. The interaction energy of two molecules was calculated as the sum of the Coulombic and Lennard-Jones interactions of all of their atom pairs. All interactions have been truncated to zero at the molecular centre–centre distance of 12.5 Å. The long-range part of the electrostatic interactions has been accounted for by the reaction field correction method [44, 45], using conducting boundary conditions (i.e. the dielectric constant of the continuum beyond the cut-off sphere of the molecules is assumed to be infinite). In order to test whether the results are dependent on the treatment of the long-range part of the electrostatic interactions, we have repeated all the calculations by setting the dielectric constant of this background continuum to unity instead of infinity (i.e. without using long-range correction). The obtained results have always been in a good qualitative agreement with those obtained under conducting boundary conditions, indicating their insensitivity to the long-range treatment of the electrostatic interactions. In the following, only the results obtained under conducting boundary conditions are presented.

The simulations were performed using the program MMC [46]. For preparing the initial configurations, the neat liquid phases of water, CCl_4 and DCE were simulated first by placing the required number of molecules into three cubic simulation boxes of the edge lengths of 25.216 Å, and equilibrating them by performing 10^8 Monte Carlo moves in each box. Then, for preparing the water/vapour system, the X edge of the water box was doubled, whereas the liquid/liquid interfacial systems were created by attaching the water box to that of the corresponding organic liquid. In each step of the simulations a randomly chosen molecule was randomly translated and rotated around a randomly chosen space-fixed axis by no more than 0.25 Å and 30°, respectively. About 30% of the tried moves have been accepted in every case. The interfacial systems were equilibrated by performing another 10^8 Monte Carlo moves in each of them. Then 5000 sample configurations per system, separated by 10^5 Monte Carlo moves each, were saved for the analyses. Finally, the sample configurations were translated along the interface normal axis X in such a way that the centre-of-mass of the 536 water molecules was placed at $X = \pm 25.216$ Å, i.e. at the boundary of the box along the X axis, in order to avoid artificial broadening of the interface due to its translation along the X axis in the simulation.

3. Results and discussion

The molecular number density profile of water, CCl_4 and DCE across the three systems simulated are shown in figure 1. In order to compare the density profiles of the organic molecules without the factor resulting from the difference in the number of CCl_4 and DCE molecules simulated, their $\rho_{org}(X)$ density profiles are normalized by the number of organic molecules present in the simulation box N_{org}. As is seen, both the water density profiles $\rho_w(X)$ and the $\rho_{org}(X)/N_{org}$ profiles are very similar to each other in the systems simulated, indicating that the structure of the interface does not depend noticeably on the composition of the apolar phase.

In order to investigate the dependence of the properties of the hydrogen bonds between the water molecules on the distance from the interface, we have divided the interfacial region of the aqueous phase into four separate layers, in which the subsequent analyses are performed separately. Layer A, covering the X range from where $\rho_w(X)$ becomes different from zero up to where it reaches 10% of the bulk density value, contains the water molecules penetrated farthest into the apolar phase. Layer B is located at the X range in which $\rho_w(X)$ is between 10% and 50% of the bulk phase water density, whereas layer C is extended to the X value where the density of water reaches its bulk value. These three layers contain the interfacial

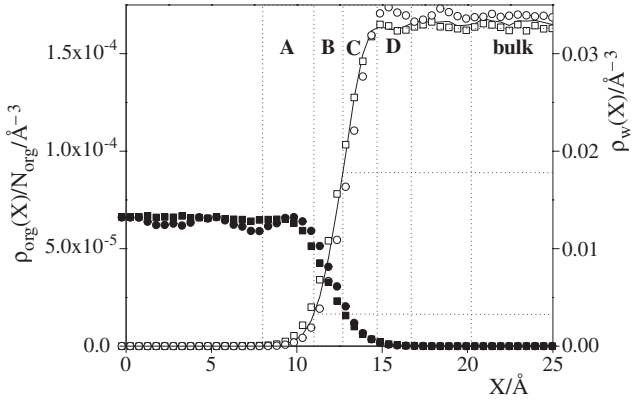

Figure 1. Number density profile of the water O atoms (open symbols) and centre-of-masses of the organic molecules (full symbols) across the simulated water/apolar liquid–liquid interfaces. The density of the organic molecules is normalized by the number of organic molecules in the basic simulation box N_{org}. Circles: water/CCl_4 system, squares: water/DCE system. The solid curve shows the density profile of the water O atoms across the system containing the water/vapour interface. All profiles are averaged over the two interfaces present in the system. The scale on the left refers to the density of the organic molecules, whereas that on the right to the water density. The dashed vertical lines show the division of the interface into four separate interfacial regions as well as the definition of the bulk water layer, whereas the dashed horizontal lines illustrate the definition of the interfacial layers in the case of the water/vapour system.

water molecules, whereas layer D, defined to be as wide as layer C, covers the subsurface water layer. It should be noted that, due to the minor differences of the water density profiles obtained in the different systems, the boundaries of the water layers defined above also vary slightly from system to system. In order to compare the results with those obtained in bulk-like water unperturbed by the interface, we have also defined a layer of bulk water as the 5 Å wide layer of the aqueous phase located farthest from the interface. (Obviously, as for the four interfacial layers, the bulk water layer is also defined in both sides of the apolar phase.) The boundaries of the four interfacial layers and that of the bulk water layer as well as the densities determining the interfacial layers are also indicated in figure 1 in the example of the water/vapour system.

In analysing the hydrogen bonding structure of water we use a combined geometric and energetic criterion for the definition of the hydrogen bond. Thus, two water molecules are regarded as being hydrogen bonded to each other upon the simultaneous fulfilment of the following three conditions: (i) the two O atoms are closer to each other than 3.35 Å, (ii) the distance of their closest intermolecular O–H pair is less than 2.45 Å and (iii) the pair interaction energy of the two molecules is below -11.5 kJ mol^{-1}. The limiting values used in this definition correspond to the position of the first minimum of the O–O and O–H partial pair correlation functions (figure 2), and to the minimum of the water pair energy distribution function (figure 3), respectively.

The atom–atom partial pair correlation functions and the distribution of the pair interaction energy $P(U_{ij})$ of water in the four interfacial layers of the three systems simulated are shown in figures 2 and 3, respectively. For comparisons, the results obtained in the bulk water layer are also shown. It should be noted that, besides the two-particle correlations, the pair correlation functions are reflecting also the change of the density of the particles in inhomogeneous systems. In fact, the partial pair correlation function of the atoms of type α and β $g_{\alpha\beta}(r)$ is defined as $g_{\alpha\beta}(r) = \rho_{\alpha\beta}(r)/\rho_\beta$, where $\rho_{\alpha\beta}(r)$ is the density of β type atoms at the distance r from an atom of type α, whereas ρ_β is the average density of the β type atoms in the entire

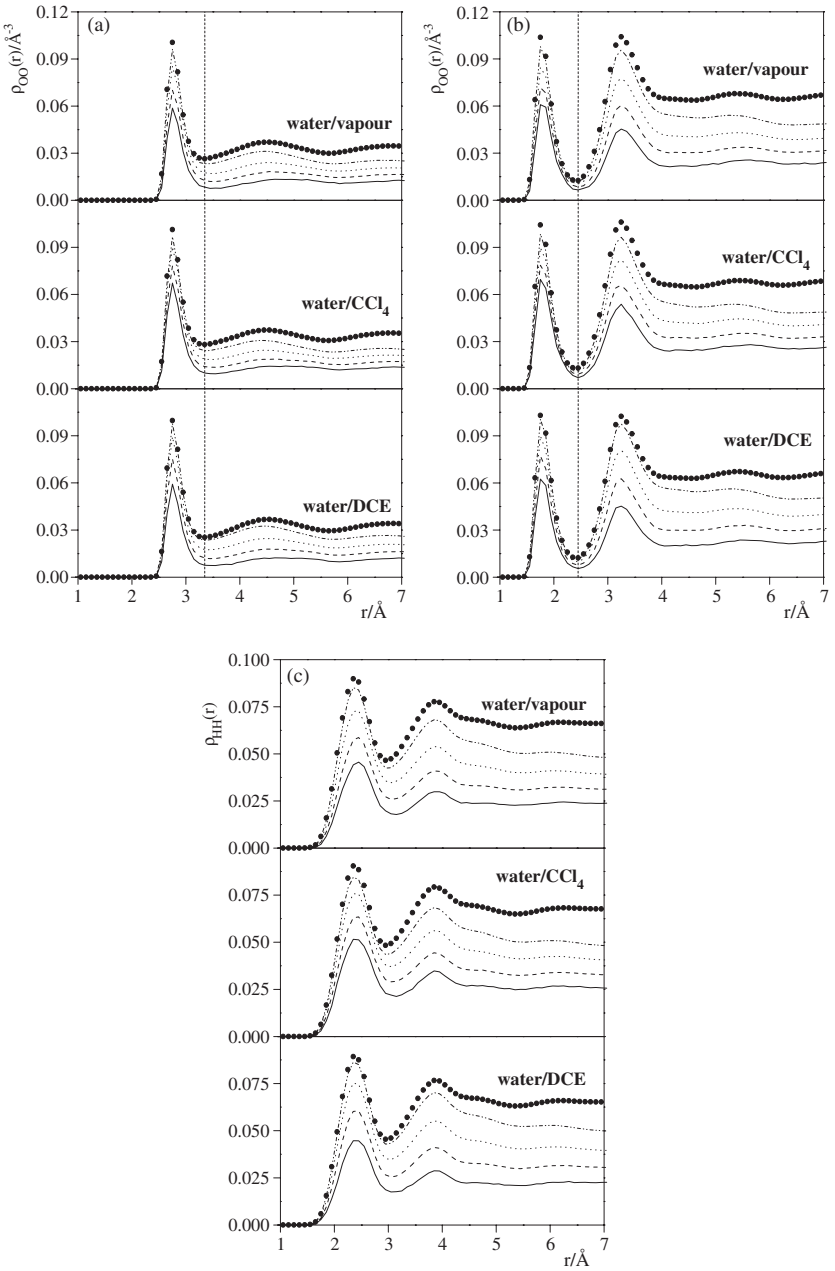

Figure 2. Number density of water atoms at a distance r from other water atoms (i.e. atom–atom partial correlation functions of water without normalizing by the density of the given atom) in the interfacial layer A (solid curves), B (dashed curves), C (dotted curves) and D (dash–dotted curves) and in the bulk water layer (full circles) of the water/vapour (top), water/CCl_4 (middle) and water/DCE (bottom) interfacial systems. (a) O atoms around O atoms, (b) O atoms around H atoms, (c) H atoms around H atoms. The dashed vertical lines show the limiting O–O and O–H distances of 3.35 and 2.45 Å, respectively, below which a water pair can be regarded as hydrogen bonded.

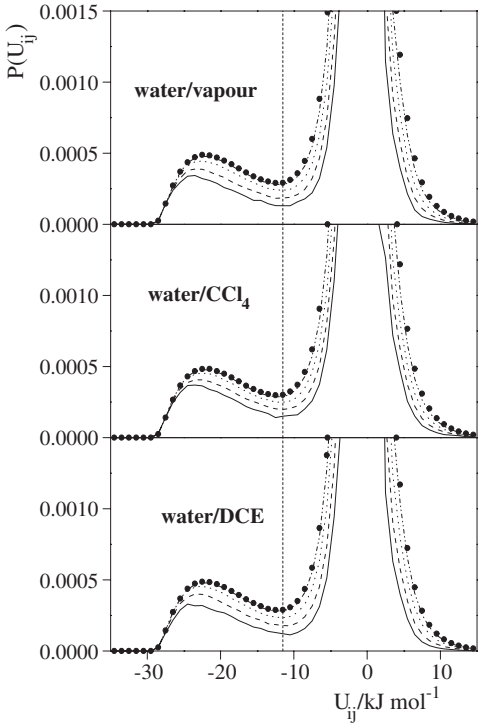

Figure 3. Distribution of the interaction energy of a water molecule located in the interfacial layer A (solid curves), B (dashed curves), C (dotted curves) and D (dash–dotted curves) and in the bulk water layer (full circles) with the other water molecules of the water/vapour (top), water/CCl_4 (middle) and water/DCE (bottom) interfacial systems. The dashed vertical line shows the limiting pair interaction energy value of -11.5 kJ mol^{-1}, below which a water pair can be regarded as hydrogen bonded.

system. However, in inhomogeneous systems, like the interfacial systems analysed here, such an average density value is meaningless, and the improper normalization of $g_{\alpha\beta}(r)$ results in large differences in its amplitude when calculated in regions of different densities. Therefore, in this study the pair correlation functions are presented without normalization, i.e. in the form of $\rho_{\alpha\beta}(r)$ instead of $g_{\alpha\beta}(r)$.

As is seen from figures 2 and 3, both the $\rho_{\alpha\beta}(r)$ and $P(U_{ij})$ functions look rather similar in the different layers of the systems simulated. The positions of the peaks and minima do not change noticeably upon getting closer to the interface. Thus, the equilibrium distance of the hydrogen bonding O atoms and that of the acceptor O and bonding H atoms is always found to be 2.75 and 1.75 Å, respectively, whereas the peak of the pair interaction energy of the H-bonded water pairs is centred at about -23 kJ mol^{-1} in each case. This finding is in clear accordance with the results of several former studies, from which it has been concluded that the water–water structure is not influenced noticeably by the presence of the interface [23, 26, 32]. However, such a comparison seems to be insensitive to small changes of the hydrogen bonding structure of water even if these changes exhibit some tendencies. In the following, we are analysing these changes in detail.

3.1. Geometry and energy of the hydrogen bonded water pairs

The distribution of the pair interaction energy of the hydrogen bonded water pairs U_{ij}^{HB} in the four interfacial regions and in the bulk water layer of the three systems simulated are shown

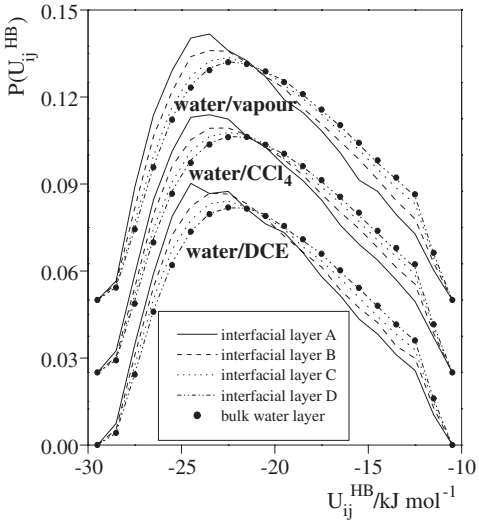

Figure 4. Distribution of the interaction energy of a water molecule located in the interfacial layer A (solid curves), B (dashed curves), C (dotted curves) and D (dash–dotted curves) and in the bulk water layer (full circles) with its hydrogen bonded neighbours in the three systems simulated. Results for the water/CCl_4 and water/vapour interfaces are shifted by 0.025 and 0.05 units, respectively.

in figure 4. As is seen, upon approaching the interface the entire distribution is gradually shifted to lower energy values in each system. Correspondingly, the position of the peak of the distribution is also shifted from the value of -22 kJ mol^{-1}, observed in the bulk water layer, by about 10% to -24 kJ mol^{-1} in the interfacial layer A. This result clearly points out that the water–water hydrogen bonds are, on average, stronger at the vicinity of an apolar interface than in the bulk liquid phase. Surprisingly, this shift of the pair interaction energy distribution is not accompanied by such evident changes in the geometry of the hydrogen bonded water pairs. The distributions of the distance between the two O atoms $r_{\mathrm{OO}}^{\mathrm{HB}}$ and between the H-acceptor O and bonding H atoms $r_{\mathrm{OH}}^{\mathrm{HB}}$ of such water pairs are shown in figures 5(a) and (b), respectively; whereas the cosine distributions of the H–O$\cdots$O angle γ of the water–water hydrogen bonds (i.e. the angle formed by the O–H chemical bond of the H-donor molecule and the O$\cdots$O axis of the hydrogen bond) are plotted in figure 6 as obtained in the four interfacial regions and in the bulk water layer of the three systems simulated. All distributions look remarkably similar to each other in each system, independently from the distance of the corresponding layer from the interface. However, when calculating the difference of the distributions obtained in an interfacial and in the bulk water layer, some small but tendentious changes are revealed. Thus, figures 5 and 6 also show the $\Delta P(x)$ differential distributions of the corresponding geometrical parameter x (i.e. x being $r_{\mathrm{OO}}^{\mathrm{HB}}$, $r_{\mathrm{OH}}^{\mathrm{HB}}$ or γ) in the four interfacial layers of the three systems studied, where $\Delta P(x) = P^{\mathrm{i}}(x) - P^{\mathrm{b}}(x)$; $P^{\mathrm{i}}(x)$ and $P^{\mathrm{b}}(x)$ being the distributions in the corresponding interfacial and in the bulk water layer, respectively. The comparison of the differential distance distributions even show some differences between the three systems investigated. Thus in the water/vapour system both the $\Delta P(r_{\mathrm{OO}}^{\mathrm{HB}})$ and $\Delta P(r_{\mathrm{OH}}^{\mathrm{HB}})$ differential distributions have a negative loop at the low r side, followed by a positive loop at the high r side of the peak of the full distribution, whereas the differential distributions are zero at the position of the peak of the full distribution. This finding indicates a slight average elongation of the hydrogen bonds upon approaching the vapour phase, without changing the equilibrium value of the O–O and O–H distances. A similar, but considerably weaker, effect is seen in the case of the water/CCl_4

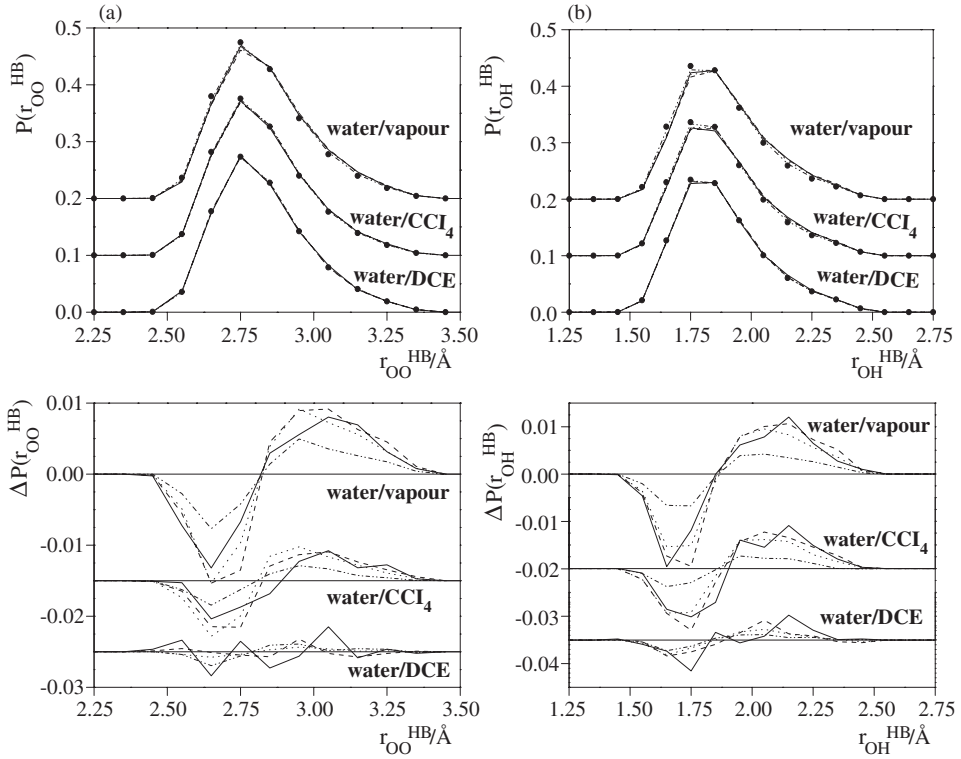

Figure 5. Distribution of (a) the O···O and (b) the O···H distance of hydrogen bonding water pairs r_{OO}^{HB} and r_{OH}^{HB}, respectively, in the four interfacial layers and in the bulk water layer of the three systems simulated (top), and the difference in the distributions obtained in an interfacial and in the bulk water layer (bottom). Solid curves: layer A; dashed curves: layer B; dotted curves: layer C; dash–dotted curves: layer D; full circles: bulk water layer. The full distributions obtained in the water/CCl_4 and water/vapour interfaces are shifted by 0.1 and 0.2 units, respectively, whereas the differential distributions of r_{OO}^{HB} in the water/CCl_4 and water/DCE systems are shifted by -0.015 and -0.025 units, and those of r_{OH}^{HB} by -0.02 and -0.035 units, respectively.

interface, i.e. when the vapour phase is substituted by an apolar condensed phase. Furthermore, when the dielectric constant of the condensed phase is somewhat increased (i.e. from about 2 to 10 [39]), this effect is washed out almost completely, as no clear tendency can be observed in the change of the hydrogen bond distances at the water/DCE interface. Interestingly, the change of the hydrogen bond angle is found to be independent from the composition of the apolar phase, as the obtained $\Delta P(\cos\gamma)$ differential cosine distributions look rather similar in the three systems investigated. These distributions have a broad positive peak between about 0.8 and 0.95 (corresponding to 36° and 18°, respectively), followed by a sharp negative peak above 0.95. This result indicates that at the vicinity of the interface the hydrogen bonds are, on average, slightly more bent than in bulk water, as the population of the hydrogen bonds characterized by an angle larger than 18° is somewhat, by about 0.5–4%, larger, at the expense of the population of the hydrogen bonds more linear than 18°, in the interfacial water layers than in bulk water.

The obtained results on the change of the geometry of the hydrogen bonded water pairs seem not to be in full accordance with those on the dependence of the pair interaction energy on the distance from the interface. One can expect that small changes in the geometry correspond

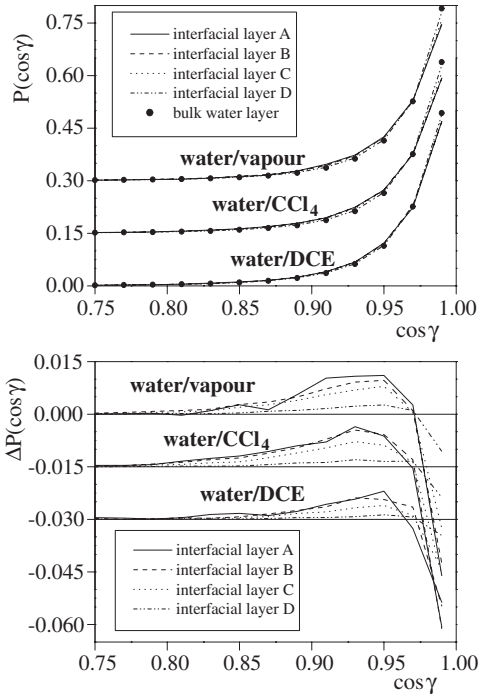

Figure 6. Cosine distribution of the H–O· · ·O angle γ of the hydrogen bonds in the four interfacial layers and in the bulk water layer of the three systems simulated (top), and the difference in the distributions obtained in an interfacial and in the bulk water layer (bottom). Solid curves: layer A; dashed curves: layer B; dotted curves: layer C; dash–dotted curves: layer D; full circles: bulk water layer. The full distributions obtained in the water/CCl_4 and water/vapour interfaces are shifted by 0.15 and 0.3 units, respectively, whereas the differential distributions in the water/CCl_4 and water/DCE systems are shifted by -0.015 and -0.03 units, respectively.

to similarly small changes in the energy of the hydrogen bonded pairs. Furthermore, the fact that the hydrogen bonds become, on average, slightly less linear at the vicinity of the interface is generally expected to imply weakening rather than strengthening of the hydrogen bonds. In order to fully understand the obtained results, we have to consider the fact that in hydrogen bonding liquids the H-bonded molecule pairs are typically much closer to each other than the optimal distance of their Lennard-Jones interactions. Thus, in such liquids the entire Lennard-Jones contribution to the total energy of the system is often repulsive [47, 48]. Considering the rapid increase of the Lennard-Jones repulsion with decreasing interatomic distances, and also our above finding that at the vicinity of the interface the population of the hydrogen bonds corresponding to the lowest interatomic distances decreases, the increasing attraction of the interfacial hydrogen bonded water pairs can be attributed to this decrease in the population of the closest approaching molecule pairs, which are characterized by the largest Lennard-Jones repulsion. Thus the energy gain corresponding to this change can overcompensate the energy cost of the slight extra bending of the hydrogen bonds, and result in the observed average lowering of the pair interaction energy of the hydrogen bonded water pairs at the vicinity of the interface.

3.2. Spatial arrangement of the neighbouring water molecules

The spatial arrangement of the neighbouring water molecules around each other can be characterized by the O· · ·O· · ·O angle θ formed by the O atoms of two neighbouring molecules

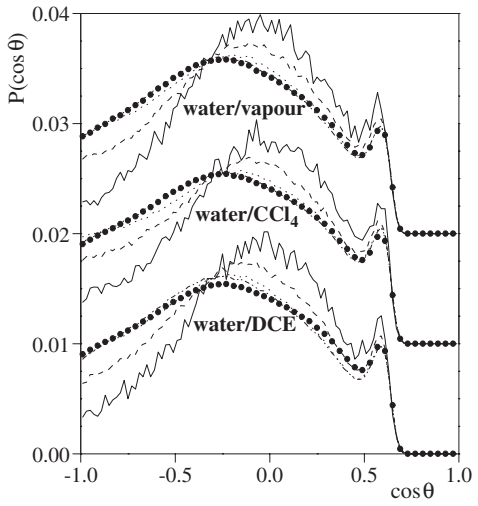

Figure 7. Cosine distribution of the angle θ formed by the O atoms of two neighbouring water molecules around the O atom of a water molecule located in the interfacial layer A (solid curves), B (dashed curves), C (dotted curves) and D (dash–dotted curves) and in the bulk water layer (full circles) of the three systems simulated. Results for the water/CCl_4 and water/vapour interfaces are shifted by 0.01 and 0.02 units, respectively.

around the O atom of the central molecule. (The term 'neighbouring' refers to water molecules having their O atoms closer to each other than 3.35 Å.) The cosine distributions of θ are shown in figure 7 as obtained in the four interfacial regions and in the bulk water layer of the three systems simulated. In bulk water $P(\cos\theta)$ is a bimodal distribution, having a large, broad peak at about -0.3, corresponding roughly to the tetrahedral angle, and a small but sharp peak at 0.5, corresponding to the angular value of 60°. The first peak is given by the tetrahedrally arranged hydrogen bonded neighbours, whereas the small peak at 0.5 is due to the interstitial neighbours, which are off the tetrahedral hydrogen bonded network, located in its cavities, and forming closely packed structures with their neighbours [49–51]. Such closely packed patches can be characterized by equilateral triangles formed by the neighbouring molecules. As is seen from figure 7, upon approaching the interface the probability of finding triplets characterized by a θ value larger than the tetrahedral angle decreases, whereas that of triplets corresponding to smaller θ angles increases rather strongly in each system studied. It is also evident that the effect of the presence of the interface, unlike that of the change of the temperature or pressure [51, 52], does not simply change the population of the hydrogen bonded and interstitial neighbours, but it reduces the population of the pairs of neighbours arranged by forming large angles around the central molecule instead. The reason for this behaviour is that the presence of the interface excludes a certain radial volume element around a nearby water molecule by preventing other molecules from accessing this space. Upon getting closer to the interface this excluded radial volume element becomes larger, which increasingly reduces the possibility of two neighbouring water molecules forming large angles around the central molecule.

3.3. Hydrogen bond statistics

Figure 8 shows the f_i fraction of the water molecules having exactly i hydrogen bonded neighbours in the four interfacial regions and in the bulk water layer of the three systems simulated. As is seen, the entire f_i distribution shifts strongly to smaller values upon

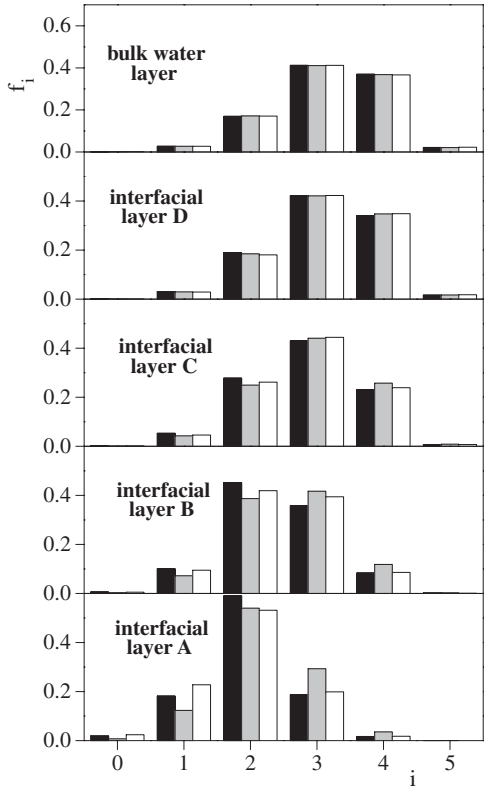

Figure 8. Fraction of the water molecules having exactly i hydrogen bonded neighbours in the interfacial layer A (bottom panel), B (fourth panel), C (third panel) and D (second panel) and in the bulk water layer (top panel) of the three interfacial systems simulated. Black columns: water/vapour system; grey columns: water/CCl_4 system; white columns: water/DCE system.

approaching the interface, indicating a clear decrease of the number of the hydrogen bonded neighbours of the molecules. Thus, while in the bulk water layer the molecules have three or four hydrogen bonded neighbours with the highest probabilities, the f_4 fraction becomes roughly equal to f_2 in the interfacial layer C, to f_1 in layer B, and to f_0 in layer A. Simultaneously with the gradual vanishing of the f_4 fraction, f_2 becomes the most populated fraction at the vicinity of the interface. Thus, in layer A about half of the water molecules have two hydrogen bonded neighbours. The reason for this decrease of the number of hydrogen bonded neighbours is again the fact that the directions from which a water molecule located close to the interface can be surrounded by water neighbours is restricted by the radial volume element excluded by the interface around this water molecule.

This effect is further illustrated by table 1, listing the average number of the hydrogen bonded neighbours as well as that of the nearest neighbours (i.e. neighbours within the O–O distance of 3.35 Å) N_{HB} and N_{NN}, respectively, of the water molecules in the four interfacial regions and in the bulk water layer of the three systems simulated. The fraction of the hydrogen bonded neighbours among the nearest neighbours N_{HB}/N_{NN} is also included in the table. As is seen, the number of both the hydrogen bonded and nearest neighbours decreases upon approaching the interface, however, in accordance with the results of several earlier studies [21, 23, 30, 32, 35], this decrease is found to be noticeably faster in the latter

Table 1. Number of nearest (coordinating) and hydrogen bonded neighbours (N_{NN} and N_{HB}, respectively) of the water molecules, as well as their ratio N_{HB}/N_{NN}, as obtained in the four separate interfacial regions and in the bulk water layer of the three systems simulated.

		Interfacial layer				Bulk water
		A	B	C	D	layer
Water/vapour	N_{NN}	2.608	3.015	3.718	4.266	4.498
	N_{HB}	2.387	2.416	2.854	3.118	3.187
	N_{HB}/N_{NN}	0.915	0.801	0.768	0.731	0.709
Water/CCl_4	N_{NN}	2.727	3.295	3.907	4.406	4.592
	N_{HB}	2.229	2.583	2.935	3.144	3.185
	N_{HB}/N_{NN}	0.817	0.784	0.751	0.714	0.694
Water/DCE	N_{NN}	2.326	3.076	3.787	4.305	4.430
	N_{HB}	1.959	2.464	2.894	3.135	3.182
	N_{HB}/N_{NN}	0.842	0.801	0.764	0.728	0.718

case. Thus, the fraction of the hydrogen bonded neighbours among the nearest neighbours increases monotonously upon getting closer to the interface. This increase of the fraction of the hydrogen bonded neighbours implies the decrease of the fraction of the interstitial neighbours and indicates that, similar to the hydration of smaller hydrophobic solutes, the overall structure of water becomes increasingly tetrahedral in the vicinity of interfaces formed by water with an apolar phase.

4. Summary and conclusions

In this paper we have presented a comprehensive analysis of the hydrogen bonding structure of water in the vicinity of interfaces with various apolar phases. The obtained results have shown that the composition of the apolar phase has rather little effect on these properties. The comparison of the distributions of the hydrogen bonding distances as obtained in layers located at different distances from the interface has revealed that upon getting closer to the interface the hydrogen bonds become, on average, slightly more elongated as the population of the shortest hydrogen bonds decreases. Since the water pairs of such short hydrogen bonds correspond to the largest Lennard-Jones repulsions, this slight change of the hydrogen bond lengths is accompanied by a considerably larger shift of the average interaction energy of the hydrogen bonded water pairs to lower energies, even if the hydrogen bonds are also slightly more bent at the vicinity of the interface than in bulk water.

It has also been found that, due to the increasing radial volume element excluded by the interface from the neighbouring water molecules, the probability that two neighbouring molecules form large angles around the central molecule becomes smaller, while the number of both the coordinating (i.e. belonging to the first O–O coordination shell) and hydrogen bonding neighbours decreases upon approaching the interface. It has also been seen that the number of the coordinating neighbours decreases noticeably faster than that of the hydrogen bonding neighbours, indicating that the overall structure of water is more tetrahedral at the vicinity of apolar interfaces than in the bulk liquid phase.

Acknowledgment

PJ is a Békésy György fellow of the Hungarian Ministry of Education, which is gratefully acknowledged.

References

[1] Frank H S and Evans M W 1945 *J. Chem. Phys.* **13** 507
[2] Lum K, Chandler D and Weeks J D 1999 *J. Phys. Chem.* B **103** 4570
[3] Turner J and Soper A K 1994 *J. Chem. Phys.* **101** 6116
[4] Polydorou N G, Wicks J D and Turner J Z 1997 *J. Chem. Phys.* **107** 197
[5] Dixit S, Crain J, Poon W C K, Finney J L and Soper A K 2002 *Nature* **416** 829
[6] Stone M T, in't Veld P J, Lu Y and Sanchez I C 2002 *Mol. Phys.* **100** 2773
[7] García-Tarrés L and Guàrdia E 1998 *J. Phys. Chem.* B **102** 7448
[8] Madan B and Sharp K 1999 *Biophys. Chem.* **78** 33
[9] Chau P L 2001 *Mol. Phys.* **99** 1289
[10] De Grandis V, Gallo P and Rovere M 2003 *J. Chem. Phys.* **118** 3646
[11] Tsuyumoto I, Noguchi N, Kitamori T and Sawada T 1998 *J. Phys. Chem.* B **102** 2684
[12] Gragson D E and Richmond G L 1998 *J. Phys. Chem.* B **102** 3847
[13] Mitrinovic D M, Zhang Z, Williams S M, Huang Z and Schlossman M L 1999 *J. Phys. Chem.* B **103** 1779
[14] Miranda P B and Shen Y R 1999 *J. Phys. Chem.* B **103** 3292
[15] Fordyce A J, Bullock W J, Timson A J, Hasalam S, Spencer-Smith R D, Alexander A and Frey J G 2001 *Mol. Phys.* **99** 677
[16] Furutaka S and Ikawa S 2001 *Fluid Phase Equilib.* **185** 379
[17] Brown M G, Walker D S, Raymond E A and Richmond G L 2003 *J. Phys. Chem.* B **107** 237
[18] Raymond E A, Tarbuck T L, Brown M G and Richmond G L 2003 *J. Phys. Chem.* B **107** 546
[19] Morita A and Hynes J T 2000 *Chem. Phys.* **258** 371
[20] Morita A and Hynes J T 2002 *J. Phys. Chem.* B **106** 673
[21] Linse P 1987 *J. Chem. Phys.* **86** 4177
[22] Wilson M A, Pohorille A and Pratt L R 1988 *J. Chem. Phys.* **88** 3281
[23] Benjamin I 1992 *J. Chem. Phys.* **97** 1432
[24] Matsumoto M, Takaoka Y and Kataoka Y 1993 *J. Chem. Phys.* **98** 1464
[25] Zhang Y, Feller S E, Brooks B R and Pastor R W 1995 *J. Chem. Phys.* **103** 10252
[26] Chang T M and Dang L X 1996 *J. Chem. Phys.* **104** 6772
[27] Taylor R S, Dang L X and Garrett B C 1996 *J. Phys. Chem.* **100** 11720
[28] Tarek M, Tobias D J and Klein M L 1996 *J. Chem. Soc. Faraday Trans.* **92** 559
[29] Wilson M A and Pohorille A 1997 *J. Phys. Chem.* B **101** 3130
[30] Benjamin I 1999 *J. Chem. Phys.* **110** 8070
[31] Dang L X 1999 *J. Chem. Phys.* **110** 10113
[32] Fernandes P A, Cordeiro M N D S and Gomes J A N F 1999 *J. Phys. Chem.* B **103** 6290
[33] Jedlovszky P, Vincze Á and Horvai G 2002 *J. Chem. Phys.* **117** 2271
[34] Jedlovszky P, Varga I and Gilányi T 2003 *J. Chem. Phys.* **119** 1731
[35] Patel H A, Nauman E B and Garde S 2003 *J. Chem. Phys.* **119** 9199
[36] Jedlovszky P, Vincze Á and Horvai G 2004 *J. Mol. Liq.* **109** 99
[37] Jedlovszky P, Vincze Á and Horvai G 2004 *Phys. Chem. Chem. Phys.* **6** 1874
[38] Jedlovszky P, Varga I and Gilányi T 2004 *J. Chem. Phys.* at press
[39] Lide D R (ed) 1994–95 *CRC Handbook of Chemistry and Physics* 75th edn (Boca Raton, FL: CRC Press)
[40] Berendsen H J C, Grigera J R and Straatsma T P 1987 *J. Phys. Chem.* **91** 6269
[41] Jorgensen W L, Chandrasekhar J, Madura J D, Impey R W and Klein M L 1983 *J. Chem. Phys.* **79** 926
[42] Kato M, Abe I and Taniguchi Y 1999 *J. Chem. Phys.* **110** 11982
[43] McDonald I R, Bounds D G and Klein M L 1982 *Mol. Phys.* **45** 521
[44] Barker J A and Watts R O 1973 *Mol. Phys.* **26** 789
[45] Neumann M 1985 *J. Chem. Phys.* **82** 5663
[46] Mezei M *MMC program*— URL: http://fulcrum.physbio.mssm.edu/~mezei/mmc
[47] Jedlovszky P and Vallauri R 1997 *Mol. Phys.* **92** 331
[48] Jedlovszky P and Vallauri R 1997 *J. Chem. Phys.* **107** 10166
[49] Svishchev I M and Kusalik P G 1993 *J. Chem. Phys.* **99** 3049
[50] Jedlovszky P, Bakó I, Pálinkás G, Radnai T and Soper A K 1996 *J. Chem. Phys.* **105** 245
[51] Jedlovszky P, Mezei M and Vallauri R 2000 *Chem. Phys. Lett.* **318** 155
[52] Jedlovszky P and Vallauri R 2001 *J. Chem. Phys.* **115** 3750